Received: 15 May 2023 | Revised: 19 June 2023 | Accepted: 3 July 2023

DOI: 10.1002/agt2.385

Aggregate Open Access WILEY

RESEARCH ARTICLE

Investigating oil solubilization into nonionic micelles by Raman multivariate curve resolution

Ciera M. Wentworth[1] | **Ryan L. Myers**[1] | **Paul S. Cremer**[1,2] | **Lauren D. Zarzar**[1,3,4]

[1]Department of Chemistry, The Pennsylvania State University, University Park, Pennsylvania, USA

[2]Department of Biochemistry and Molecular Biology, The Pennsylvania State University, University Park, Pennsylvania, USA

[3]Department of Materials Science and Engineering, The Pennsylvania State University, University Park, Pennsylvania, USA

[4]Materials Research Institute, The Pennsylvania State University, University Park, Pennsylvania, USA

Correspondence
Lauren D. Zarzar and Paul S. Cremer, Department of Chemistry, The Pennsylvania State University, University Park, PA 16802, USA.
Email: ldz4@psu.edu; psc11@psu.edu

Funding information
Army Research Office, Grant/Award Number: W911NF-18-1-0414; David and Lucile Packard Foundation, Grant/Award Number: 2019-69664; National Science Foundation, Grant/Award Number: CHE-2004050

Abstract

Hydrophobic hydration, whereby water spontaneously structures around hydrophobic and amphiphilic molecules, plays a key role in the process of surfactant micelle formation and micellar oil solubilization. Using vibrational Raman multivariate curve resolution spectroscopy, we characterized changes in the hydrophobic hydration occurring within nonionic alkylphenol ethoxylate surfactant Tergitol NP-12 micelles as a function of oil solubilization. We report trends in the changes of hydrophobic hydration depending on the chain length of the oil as well as the presence of a halogen atom in the oil chemical structure. Changes in hydrophobic hydration directly correlate to changes in the physical properties of the micellar solution, including cloud point and micelle hydrodynamic diameter. We compare hydrophobic hydration of Tergitol NP-12 to nonionic linear alkyl ethoxylate surfactant Makon TD-12 and ionic sodium dodecyl sulfate and observe similar trends; the molecular structure of the oil has the largest impact on the hydrophobic hydration. We believe these studies contribute to a fundamental understanding of the importance of hydrophobic hydration in surfactant and oil aggregates, especially as it relates to micellar oil solubilization, and provide insight into how the molecular solubilizate can impact micellar structure, size, and stability.

KEYWORDS
hydrophobic hydration, micelle, Raman multivariate curve resolution, solubilization

1 | INTRODUCTION

Surfactants are amphiphilic molecules that stabilize interfaces by lowering the interfacial tension (γ) between two phases. For water-soluble surfactants above the critical micelle concentration (CMC), surfactant monomers aggregate into nanometer-sized structures called micelles due to the hydrophobic effect.[1,2] For micelles formed in water, the micelle contains a hydrophilic exterior and a hydrophobic interior core into which hydrophobic molecules can be partitioned. Surfactants and micelles are thus widely used in research and application involved in cleaning,[3,4] dispersing,[5,6] mixing,[7–9] and chemical separations.[10–12] Hydrophobic hydration is a phenomenon in which hydrophobic or amphiphilic molecules induce spontaneous structuring of water.[13,14] Hydrophobic hydration is theorized to play a fundamental role in hydrophobic interactions, which are vital to micellar oil solubilization.[15–18] Yet, there is gap in our knowledge about the hydrophobic hydration of nonionic micelles compared to the hydrophobic hydration of ionic micelles, whose charge effects between headgroups dominate their solvation and dynamics in solution.[14,19] Here, using the emerging technique of vibrational Raman multivariate curve resolution (MCR) spectroscopy, we investigate the impact of oil solubilization on the hydrophobic hydration and structure of nonionic surfactant micelles in water.

Nonionic surfactants are those in which the headgroup is polar and uncharged. These amphiphilic molecules tend to be physiologically mild and are not prone to precipitating or denaturing proteins and nucleic acids, and thus are widely used in pharmaceuticals, cosmetics, and industrial formulations. Furthermore, surfactants with polyethylene oxide (PEO) hydrophilic headgroups are chemically compatible with most water-soluble organic and inorganic compounds and remain effective over a wide range of pH values, rendering them suitable for a wide variety of uses.[20] Due to the lack of headgroup charge, it has been suggested that solubilizates (e.g., oils that are partitioned into the micelle) can be present not only in the hydrophobic core of the micelle, but at the hydrophilic-hydrophobic boundary,[21,22]

Ciera M. Wentworth and Ryan L. Myers contributed equally to this work.

as well as within the PEO palisade,[23,24] depending on the structure of the nonionic surfactant. In addition, most commercial nonionic surfactants are polydisperse, leading some authors to find, such as in the case of Triton X-100, that the micelles have overlapping internal and external surfactant molecules, leading to an ill-defined hydrophilic-hydrophobic boundary, thereby generating difficulty in identifying solubilization sites.[25] Two-dimensional nuclear Overhauser effect spectroscopy (2D NOESY) has shown that when heptane is solubilized into Triton X-100 micelles, it disrupts the layered micelle structure, oil interacts with the PEO headgroup, and the heptane dehydrates the surfactant molecules.[24] Goldenberg et al.[26] found that depending on the chemical structure, some solubilizates such as carbofuran cannot reside in the PEO palisade and are confined to the micellar core of alkylphenol ethoxylates. These results highlight the idea that solubilization is the product of a complex interaction between the surfactant and solubilizate and cannot be strictly predicted or governed by the surfactant's structural features such as the lengths of hydrophilic PEO and hydrophobic tail. The surfactant-solubilizate relationship is also heavily influenced by the properties of the solubilizate including its polarity, polarizability, lipophilicity, chain length and branching, which can impact the degree of solubilization and distribution within the micelle. Many experimental techniques and methods such as quasi-elastic light scattering, 2D NOESY, ultra violet spectroscopy, carbon-13 nuclear magnetic resonance, and solvent model systems have attempted to characterize solubilization but all have limitations in determining solubilizate location and micellar structure.[26]

Raman MCR spectroscopy is an emerging vibrational spectroscopy technique capable of identifying solute-induced perturbations of solvent molecules. When a solute is added to a solvent, typically, only the first hydration shell around the solute is affected, thereby leaving the vast majority of the solvent molecules undisturbed. Thus, when conducting vibrational spectroscopy, signal from the unperturbed solvent in the bulk tends to dominate and hides changes in the hydration layer. A home-built Raman setup was used to obtain a 1000:1 signal-to-noise ratio in order to use MCR analysis to deduce hydration information. Raman MCR has thus been employed to study the structure and hydration of ions,[27–29] small hydrophobic molecules,[30–32] polymers,[33,34] and surfactant micelles.[35,36] Since the hydrophobic effect drives the aggregation of surfactant molecules, measuring changes in the hydrophobic hydration of micelles can provide fundamental information regarding micelle structure and properties.[14] Thus far, the use of Raman MCR has been limited to studying the hydrophobic hydration of ionic surfactants and micelles, such as decyltrimethylammonium bromide and sodium octanoate.[35,36] For example, Long et al.[35] observed dangling OH peak features with ionic sodium decanoate micelle formation, suggesting that water can penetrate into the hydrophobic tail region of a micelle, hydrating up to 20% of the surfactant methylene groups; the size of these hydrated cavities also depended upon the chain length of the surfactant. Researchers also observed that when sodium decanoate and decyltrimethylammonium bromide ionic micelles are swollen with d-hexane, the oil resides in the dry oil-like core of the micelle.[35] However, one might hypothesize that the water structure around nonionic surfactant micelles with PEO headgroups, which only align water in the first hydration shell, is fundamentally different than the water structure around an ionic surfactant micelle wherein which generation of an electric field aligns subsequent waters beyond the first hydration shell.[37] By characterizing the solvated water within and around nonionic micelles, we can gain insight into hydrophobic interactions and the location of the solubilizate within the micelle.

Here we characterize the hydrophobic hydration changes of nonylphenol ethoxylate Tergitol NP-12 micelles by systematically solubilizing oils of varying lengths and halogenation (n-alkanes, n-bromoalkanes, and n-iodoalkanes). We explore the effects of oil chain length and halogenation on the oil orientation and solubilization sites within the micelle. We find that hydrophobic hydration is highly influenced by oil length, where shorter chain oils displace the most water from the micelle while longer chain oils displace a minimal amount of water from the micelle. Oil halogenation only contributes to large changes in hydrophobic hydration with shorter oil chain lengths and becomes less relevant as the chain length is extended. We compare these results to a linear alkyl ethoxylate nonionic surfactant Makon TD-12 and an ionic surfactant sodium dodecyl sulfate (SDS) and observe similar trends in hydrophobic hydration, making the solubilized oil the most significant factor in predicting hydrophobic hydration changes within the micelle. The micelle hydrodynamic diameter, solution cloud point, and micellar solubilization capacity are also quantified for each surfactant and oil condition to correlate with changes in the hydrophobic hydration. Our results suggest hydrophobic hydration changes of micellar solutions that undergo oil solubilization directly impact the micellar structure and the physical properties of the micelle.

2 | RESULTS AND DISCUSSION

We first aimed to develop a Raman MCR procedure[38] to characterize the perturbed water in and around a nonionic micelle composed of an alkylphenol ethoxylate, Tergitol NP-12. To begin, we examined the MCR spectrum of 1 wt% Tergitol NP-12 in H_2O but found extensive overlap was present between the water OH stretch from 2800–3800 cm^{-1} and the surfactant CH stretches at approximately 2700–3100 cm^{-1}. Since we needed to define a baseline using the surfactant's aromatic CH centered at ~3080 cm^{-1} (as shown in Figure 1A), this overlap made consistently defining the baseline difficult. To avoid aromatic CH/ OH stretch peak overlap, we switched to D_2O as the solvent. Deuterating the water causes the very broad OH stretch to red shift from ~3300 cm^{-1} to ~2400 cm^{-1} (OD stretch, as shown in Figure 1A), thereby allowing for more consistent baseline determination and greater signal resolution from the CH stretch region. We next wanted to determine if the contribution from dissolved surfactant monomers (as compared to the micelles) had a significant effect on the Raman signal, so we took a spectrum of 0.005 wt% Tergitol NP-12, which is below the surfactant CMC of 0.0085 wt%; we found that the OD intensity of 0.005 wt% NP-12 was near zero (Figure S1). We concluded that the surfactant monomer had no observable effect on the Raman signal, and thus any signal we measure for surfactant concentrations above the CMC is dominated by micelles. To obtain an optimal signal-to-noise

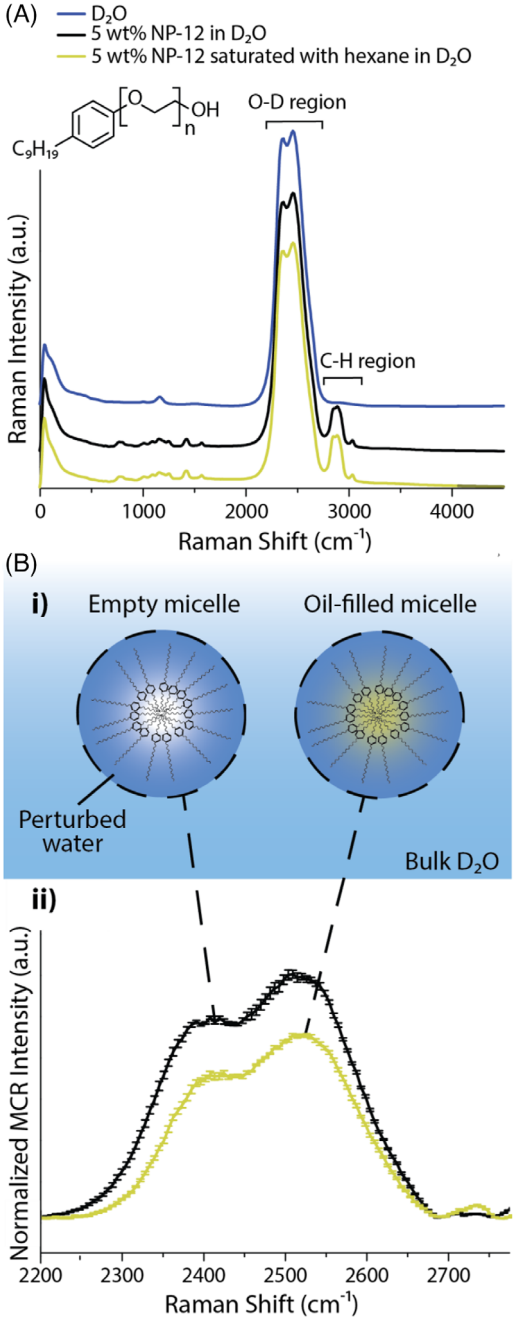

FIGURE 1 Raman multivariate curve resolution (MCR) provides insight regarding the perturbation of water within and around micelles. (A) Overlayed artificially spaced Raman spectra of pure D_2O (blue line), 5 wt% Tergitol NP-12 micelles in D_2O (black line), and 5 wt% Tergitol NP-12 micelles saturated with hexane (yellow line). Tergitol NP-12 structure is shown where *n* is an average of 12. (B-i) Schematic showing a simplified version of a Tergitol NP-12 micelle. The empty (unsaturated) micelle is on the left, where the perturbed water is shown in dark blue inside of the dashed lines, and the oil-filled (saturated micelle) is shown on the right with oil inside of the micelle. (B-ii) Normalized MCR intensity of 5 wt% Tergitol NP-12 in D_2O (black line) and 5 wt% Tergitol NP-12 micelles saturated with hexane (yellow line) showing that oil saturation of hexane into the micelle decreases the amount of perturbed water in the system (less water inside of dotted lines in the schematic). Error bars are the standard deviation of three runs.

ratio, we collected the spectra of 1, 3, and 5 wt% Tergitol NP-12 and found that 5 wt% Tergitol NP-12 yielded a strong, reproducible signal (Figure 1A). We thus used 5 wt% Tergitol NP-12 for most of the following experiments.

We next aimed to determine if there was an observable difference in the OD region between the Raman MCR spectra of empty (unsaturated) and oil-filled (saturated) 5 wt% Tergitol NP-12 micelles (Figure 1A-B). We collected a background spectrum of pure D_2O, which represents unperturbed bulk solvent (i.e., the light-blue "Bulk D_2O" region in Figure 1B-i). We then took a Raman spectrum of empty 5 wt% Tergitol NP-12 micelles, which includes signal from the micelles, bulk D_2O, and D_2O that is perturbed by solvating the micelles (i.e., the dark blue region inside the dotted line of the "empty micelle" in Figure 1B-i). We next collected the Raman spectrum of 5 wt% Tergitol NP-12 with hexane solubilized into the micelle, which contains signal from the micelle, bulk D_2O, perturbed water, and oil (Figure 1B-i). (For the oil solubilization, procedure refers to the experimental methods section in the SI). The MCR algorithm was used to deconvolute the signal from the surfactant and surfactant-perturbed water from the bulk water in the region 2200–2775 cm^{-1} spectral region (Figure 1B-ii). This allowed us to isolate changes in the micellar-solvated D_2O when transitioning from empty to oil filled micelles (comparing the dark blue water encompassed within the dotted lines of Figure 1B-i). The signal contribution from the oil in the CH region of the spectrum is expected to be minimal, since the oil is present in mM or lower concentrations, which is significantly less than the surfactant. Figure 1B-ii shows the MCR spectra of unsaturated 5 wt% Tergitol NP-12 versus hexane-saturated 5 wt% Tergitol NP-12, where we calculate a ~25% decrease in MCR area from 2200–2775 cm^{-1} when hexane is added to the micelle. This decrease indicates that when hexane is solubilized into the micelle, some of the water that previously had solvated the micelle was removed.

Having developed a protocol to investigate the hydrophobic hydration of the nonionic micelles, we then probed the impact of chain length and halogenation for the oil on the micelle hydration. We saturated 5 wt% Tergitol NP-12 micelles with n-hexane, n-octane, n-decane, and n-hexadecane. We expected significant differences in hydrophobic hydration between these samples, because previous cryo-TEM studies on Triton X-100 (a similar nonionic surfactant) revealed that alkane chain length directly impacts interactions between surfactant molecules and affects overall micelle aggregation.[39] As shown in the MCR graphs in Figure 2A, as the chain length of the alkane increases, we find that less perturbed water is removed from the micelle. Solubilization of hexane removes the most water, contributing to an MCR area decrease of 25%. By contrast, solubilization of hexadecane expels the least amount of water with only an 11% MCR area decrease.

Next, we were interested in how small changes in polarizability of the oil, such as by addition of a halogen atom, might affect the dehydration of the PEO headgroups of the Tergitol NP-12 micelle and whether a halogenated oil might have an orientation dependence within the micelle. We used MCR to analyze the perturbed water for 5 wt% Tergitol NP-12 saturated with 1-bromoalkanes and 1-iodoalkanes with carbon numbers of 6, 8, 10, and 16. Within each halogenated oil series, (bromo and iodo) we observed similar trends as for the alkanes, where the amount of expelled water decreased with increasing carbon number (Figure 2B). As shown in Figure 2B, we found that, generally, that bromoalkanes and iodoalkanes contribute to larger MCR area decreases than alkanes, with approximately 20% more displaced water (i.e., less total perturbed water) from the micelles for oils with

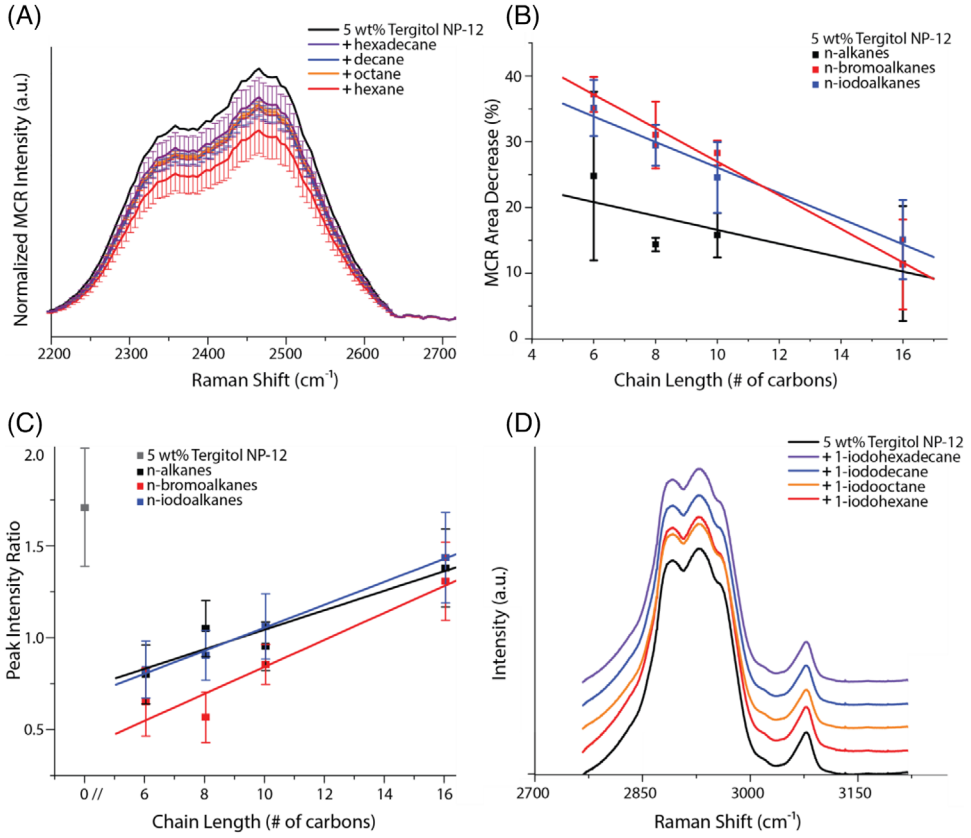

FIGURE 2 Multivariate curve resolution (MCR) analysis reveals trends in hydrophobic hydration for micelles saturated with oils of varying length and halogenation. (A) Representative MCR spectra of 5 wt% Tergitol NP-12 (black) and spectra of the processed average of four independent trials of 5 wt% Tergitol NP-12 saturated with hexadecane (violet), decane (blue), octane (orange), and hexane (red). The data were processed to display the average and standard deviation of the observed OH intensity decrease in the MCR spectra compared to the unsaturated micelle by multiplying the unsaturated micelle spectrum (black) by the average percent decrease of each oil-saturated micelle condition. The spectra were normalized to the CH region of the spectrum. (B) MCR area percent decrease of 5 wt% Tergitol NP-12 micelles saturated in n-alkanes (black), n-bromoalkanes (red), and n-iodoalkanes (blue) as a function of carbon chain length. Error bars are standard deviation of 3 trials (9 runs total). (C) The peak intensity ratio of aromatic OH (2703 cm^{-1}) to free OH (2732 cm^{-1}) of the MCR spectrum of n-alkanes (black), n-bromoalkanes (red), and n-iodoalkanes (blue) as a function of carbon chain length. Error bars are standard deviation of 3 trials (9 runs total). (D) The CH region (2800–3150 cm^{-1}) of the Tergitol NP-12 micelles as a function of n-iodoalkane chain lengths. Lines on graph have been spaced in order to aid in visualization of peaks.

carbon numbers 6 and 8. However, for a carbon number of 16, halogenation (bromo or iodo), did not have a significant impact on the dehydration of the micelle. We did not observe a significant difference in the change in hydrophobic hydration when comparing oil-filling of bromoalkanes and iodoalkanes. This was unexpected, because iodine is larger and more polarizable compared to the bromine, so one might suspect the iodoalkanes to expel more water from the micelle than bromoalkanes. Instead, we find that having a halogen moiety on the oil, compared to the alkanes, overall had a larger contribution to water expulsion than the size of the halogen.

Due to the large differences in the amount of expelled water from the micelle between oil chain lengths 6 and 16, we hypothesized that short and long chain oils solubilize differently within the micelle, with the potential for multiple solubilization sites.[21–24] We observed changes in the ratio between pi-hydrogen bonds (hydrogen on water pointing towards aromatic group, pi interaction) at 2703 cm^{-1}, and the free OH (hydrogen on water pointing towards a hydrophobic molecule) at 2732 cm^{-1} (Figure S2). For shorter oil chain lengths, the pi-hydrogen (pi-H) interaction disappears, indicating that the oil is displacing the water that was surrounding the aromatic group on Tergitol NP-12. At longer oil chain lengths, the pi-H interaction is present at similar quantities as was observed for empty micelles. In Figure 2C we have plotted the pi-H to free OH intensity ratio of the various oils added to the NP-12 micelle. The low peak intensity ratio of pi-H to free OH shows that water interacting with the pi aromatic group of the surfactant decreases, for micelles swollen with shorter chain oils (ratio below 1.0). Oils with a chain length of sixteen have the highest peak intensity ratio of 1.4 (with oil-filling) with the unsaturated micelle having a ratio of 1.7. Due to the aromatic group being directly adjacent to the PEO headgroup, these results may suggest that shorter oils, which remove water around the aromatic group, could possibly penetrate further outside of the hydrophobic core into the headgroup region of the NP-12 micelle. While longer oils, that do not remove water from the aromatic region, may be more likely sit in the hydrophobic core of the micelle and do not penetrate into the PEO headgroups. To confirm if shorter oils (that interfere with the aromatic group pi interaction) can penetrate further beyond the aromatic group into the PEO headgroup, we wanted to determine the oil's miscibility within the PEO palisade. In order to estimate the PEO solubility, we used a refractometer to extrapolate between the refractive indices of the pure bromoalkane and pure poly(ethylene glycol) (average molecular weight 200 g/mol) (PEG 200) in order to estimate volume fractions that average to the measured refractive index (refer

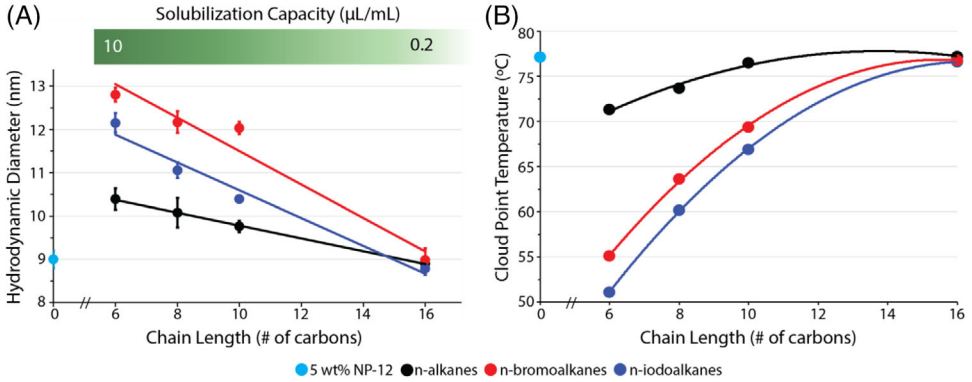

FIGURE 3 Observed trends in micelle hydrodynamic diameter, solubilization capacity, and cloud point of 5 wt% Tergitol NP-12. (A) Graph of hydrodynamic diameter of 5 wt% Tergitol NP-12 micelles versus oil chain length solubilized into the micelle, where the unsaturated empty micelle diameter is shown in cyan, micelles with n-alkanes solubilized shown in black, micelles with n-bromoalkanes solubilized shown in red, and micelles with n-iodoalkanes solubilized shown in blue. Error bars are the standard deviation of three measurements (9 runs total). The approximate range of solubilization capacity is shown above. Refer to Table S1-S2. (B) Graph of cloud point temperature of 5 wt% Tergitol NP-12 micelles versus oil chain length solubilized into the micelle, where the unsaturated empty micelle cloud point is shown in cyan, micelles with n-alkanes solubilized shown in black, micelles with n-bromoalkanes solubilized shown in red, and micelles with n-iodoalkanes solubilized shown in blue. Error bars are plotted but are encompassed in the size of the marker (error 0.1–0.2°C), error bars are standard deviation of three measurements (9 runs total). Lines on the graph are only meant to guide the eye.

to experimental methods in SI). We find that the solubility of the bromoalkanes in PEG 200 is significantly large compared to their water solubility, calculating 1.1, 0.80, 0.63, and 0.0 M for bromoalkanes with chain lengths 6, 8, 10, and 16 respectively. For short chain oils, the lack of a pi-H interaction combined with their PEO solubility suggests that it is likely that they can solubilize into the PEO palisade of the surfactant headgroup.

To determine if the halogenated oils induced any structural changes to the Tergitol NP-12 micelle or possessed any preferential orientation within the micelle, we performed high resolution (1800 gratings/mm) MCR on the CH stretch region (2700–3100 cm^{-1}) of the micelle for a series of iodoalkanes (Figure 2D). We found no change in the CH region, which signified that there was no significant change in the hydrophobic environment and observable structural modifications within the micelle or preferential oil orientation within the micelle.

We aimed to gain insight into how the hydrophobic hydration trends observed with Raman MCR correlate with physical properties of the Tergitol NP-12 micelles (e.g., micelle hydrodynamic diameter, solubilization capacity, and cloud points). We used dynamic light scattering to determine how the micelle hydrodynamic diameter changes upon oil solubilization. As shown in Figure 3A, the hydrodynamic diameter of the micelle is 9.0 ± 0.2 nm, and the hydrodynamic diameter increased significantly upon solubilization of oils with 6–10 carbons. However, for oil with 16 carbons, we did not observe a significant size change within error (Table S1 for all values). Varying the halogen atom of the oil had a small impact on the micelle hydrodynamic diameters, with the iodoalkanes yielding micelles with slightly smaller hydrodynamic diameter than the bromoalkanes. A plot showing the relationship between MCR area decrease and micelle hydrodynamic diameter is shown in Figure S3. As expected, the cloud point shows little difference between brominated and iodinated oils, but there were large differences between oils of varying chain length, where decreasing the carbon number from 16 to 6 yielding a significant reduction in the cloud point from 77.1 ± 0.2°C to below 55°C (Figure 3B). The cloud point depression for shorter chain oils was expected due to the fact it has the largest impact on hydrophobic hydration where the oil is effectively dehydrating the PEO headgroup, and a similar effect has been observed in the literature with other surfactants.[40,41] Iodoalkanes led to slightly lower cloud point temperatures, perhaps due to the greater polarizability of the iodine.

The general observations regarding micelle hydrodynamic diameter and cloud point trends mirrored the results for the changes in MCR area, where the longest chain length oils also had the least impact on the micelle structure and amount of perturbed water. We hypothesized that these trends might be related to the varying capacity of the micelles to solubilize oils of different chain lengths. We measured the approximate solubilization capacity of each oil in 5 wt% NP-12 (Table S2). Overall, we found solubilization capacity decreases as oil length increases, which is consistent with literature results.[42] Oils with 6, 8, 10, and 16 carbons have a capacity of roughly 10, 8, 5, and less than 0.2 μL/mL, respectively. For each, we calculated approximately how many oil molecules there are per micelle, using an estimated aggregation number of 100 surfactant molecules per micelle, yielding approximately 100, 70, 30, and 1 oil molecule(s) per micelle, respectively. We surmise that the higher solubilization capacity for shorter chain oils compared to that of longer chain oils may be due to the fact that the smaller oils can interact with the surfactant's PEO headgroup in addition to the hydrophobic tail, thus providing increased solubilization sites, and also leading to increases in the hydrodynamic diameter and decreasing the cloud point.[43] In contrast, longer chain oils are only solubilized within the micelle hydrophobic core, which leads to a reduced solubilization capacity and limited changes to the micelle structure and physical properties. Thus, the oil's PEO solubility may be an important factor in predicting solubilization capacity, solubilization sites, and significant changes in hydrophobic hydration with micellar oil solubilization. Molecular dynamic (MD) simulations have shown that oil molecules can reside in the surfactant headgroup in addition to the micellar core but have not explicitly explored hydrophobic hydration changes with varying oil lengths

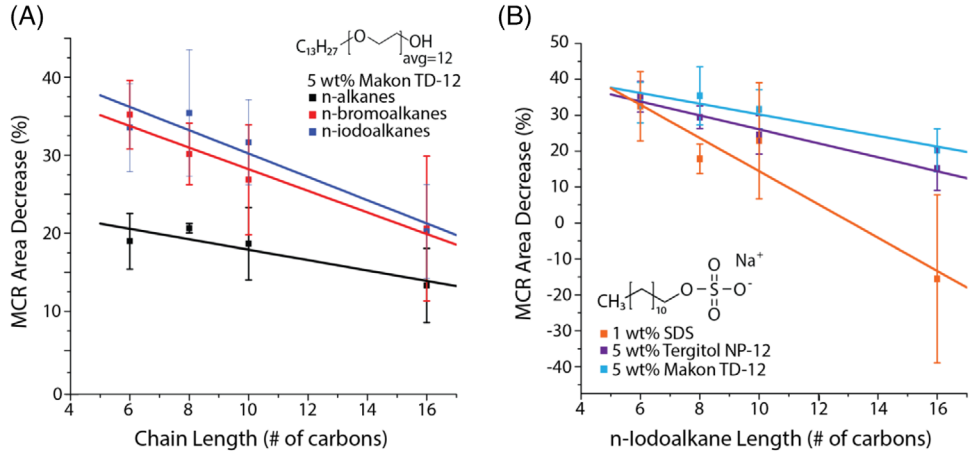

FIGURE 4 Multivariate curve resolution (MCR) analysis of different surfactants and the impact of oil solubilization on hydrophobic hydration. (A) MCR area percent decrease for 5 wt% Makon TD-12 micelles saturated with n-alkanes (black), n-bromoalkanes (red), and n-iodoalkanes (blue) as a function of carbon chain length. Error bars are standard deviation of 3 trials (9 runs total). (B) MCR area percent decrease of 1 wt% SDS (orange), 5 wt% Tergitol NP-12 (purple), and 5 wt% Makon TD-12 (light blue) as a function of n-iodoalkane length. Error bars are standard deviation of three trials (9 runs total).

and types. Further research directions could include MD simulations to characterize the role of hydrophobic hydration in micellar oil-solubilization processes.[43]

Having extensively explored the properties of the alkylphenol ethoxylate surfactant, Tergitol NP-12, we wanted to examine how changes in the surfactant chemical structure would alter the hydrophobic hydration and micellar solubilization capacity. We chose to examine an alkyl ethoxylate surfactant, Makon TD-12 (CMC = 0.013 wt%) which has the same PEO headgroup size distribution as the Tergitol NP-12 but has only a linear alkyl tail and no aromatic ring. We hypothesized that due to the absence of the aromatic group, we might observe a difference in the amount of perturbed water and impact of oil filling; however, as shown in Figure 4A, we observe similar MCR area decreases and trends to that observed for Tergitol NP-12 (Figure 2B). We also measured similar trends in the Makon TD-12 micelle hydrodynamic diameter with oil solubilization (Table S1). The measured solubilization capacity of 5 wt% Makon TD-12 was slightly less than that of Tergitol NP-12, for oils of 6, 8, 10, and 16 carbons having a capacity of roughly 6.5, 5, 3, and less than 0.2 μL/mL, respectively, but the trend remained identical (Table S2).

To contextualize our findings regarding the hydrophobic hydration and micelle structure of nonionic surfactants, we wanted to compare the results for nonionic surfactants with those of an ionic surfactant, sodium dodecyl sulfate (SDS). SDS micelles have not been characterized by Raman MCR previously, although other ionic surfactant micelles, such as sodium octanoate, sodium decanoate, and decyltrimethylammonium bromide have been studied.[35,36] As shown in Figure 4B and Figure S4, we contrast 5 wt% Tergitol NP-12, 5 wt% Makon TD-12, and 1 wt% SDS with solubilized n-iodoalkanes. We used 1 wt% SDS instead of 5 wt% SDS to obtain a clear and consistent baseline, as increasing the concentration caused baseline nonlinearity. When 1 wt% SDS micelles were saturated with 1-iodohexane, we observed an MCR area decrease of 35%, which was comparable to the results obtained for both the Tergitol NP-12 and Makon TD-12 with oil saturation of 1-iodohexane. However, for longer chain oils (8, 10, and 16), the SDS micelles had significantly less displaced water than the nonionic surfactants. Nonlinear baselines in SDS due to impurities in the surfactant created difficulty in analyzing MCR data, which lead to large errors in the MCR area percent decrease. It is not believed that the MCR area percent decrease for 1-iodohexadecane in SDS is negative, as seen in Figure 4B, which would suggest an increase in perturbed/solvated water around the oil-swollen micelle compared to the empty micelle. Instead, we attribute this result to challenges associated with the nonlinear fluorescence background of the spectrum. Overall, we observed some effect of the oil on the hydrophobic hydration changes with solubilization at short oil lengths. But due to the strong head group charge that electrostatically orders water beyond the first hydration shell, there seems to be limited solubilization ability especially as we increase the length of the iodoalkane. This could be a result of longer oils having a higher energy barrier to cross the electrostatic boundary into the core of the micelle because of the increasing hydrophobicity of the oil. We also observed little change in the hydrodynamic diameter of the SDS micelle with oil filling (Table S1).

3 | CONCLUSIONS

We have explored changes in hydrophobic hydration resulting from oil solubilization of the nonionic surfactants Tergitol NP-12, Makon TD-12, and the ionic surfactant SDS. Most prominently, we observed that short chain oils release the most water from the micelle and correspondingly affect the physical properties of the micellar solution more significantly. Longer chain oils displace little water from the micelle and do not have a significant effect on the micelles size and physical properties of the solution. The disappearance of the pi-H peak for shorter chain oils and their high PEO solubility suggested that shorter chain oils can solubilize more readily into the PEO palisade in addition to the micelle interior, while longer chain oils tend to only solubilize into the hydrophobic core, do not disrupt the water-pi interaction, and have poor PEO solubility. We also found that halogenation of the oil contributes to much larger changes in hydrophobic hydration at shorter oil lengths and does not contribute to significant changes in hydrophobic hydration at long chain

lengths. Lastly, when Tergitol NP-12 was compared to Makon TD-12 and SDS, we observed similar trends in hydrophobic hydration changes with oil length, where shorter oils displace the most water from the micelle while longer oils displace the least. These findings indicate that the oil chemical structure has a direct impact on hydrophobic hydration of the micelle, micelle stability, and micelle size. We believe these results provide insight into how solubilizate structure can be manipulated to influence micellar structure and properties as solubilization vehicles for a wide variety of technologies and applications.

ACKNOWLEDGMENTS

C. W. and L. Z. acknowledge funding support from the Army Research Office (grant number: W911NF-18-1-0414) and the David and Lucile Packard Foundation (grant number: 2019-69664). R.M. and P.C. acknowledge funding support from the National Science Foundation (grant number: CHE-2004050). The authors would also like to acknowledge Tinglu Yang for his expertise and construction of the home-built Raman experimental setup.

CONFLICT OF INTEREST STATEMENT

The authors declare no competing interests.

DATA AVAILABILITY STATEMENT

The data that support the findings of this study are available from the corresponding author upon reasonable request.

ORCID

Lauren D. Zarzar https://orcid.org/0000-0002-3287-3602

REFERENCES

1. D. Ben-Amotz, D. Mendes De Oliveira, *J. Chem. Phys.* **2021**, *155*, 224902.
2. A. Khoshnood, B. Lukanov, A. Firoozabadi, *Langmuir* **2016**, *32*, 2175.
3. M. F. Cox, *J. Am. Oil Chem. Soc.* **1986**, *63*, 559.
4. J. J. Scheibel, *J. Surfactants Deterg.* **2004**, *7*, 319.
5. Z. Zhu, X. Song, Y. Cao, B. Chen, K. Lee, B. Zhang, *Curr. Opin. Chem. Eng.* **2022**, *36*, 100770.
6. R. Prasanna Shankara, N. R. Banapurmath, A. D. Souza, S. S. Dhaded, *IOP Conf. Ser. Mater. Sci. Eng.* **2020**, *872*, 012074.
7. N. Harnby, M. F. Edwards, *Mixing in the Process Industries*, 2nd ed., Butterworth-Heinemann, Oxford, UK **1992**.
8. L. Fradette, B. Brocart, P. A. Tanguy, *Chem. Eng. Res. Des.* **2007**, *85*, 1553.
9. A. James, *Transp. Res. Circ.* **2006**, *2006*. https://onlinepubs.trb.org/onlinepubs/circulars/ec102.pdf
10. R. P. Frankewich, W. L. Hinze, *Anal. Chem.* **1994**, *66*, 944.
11. J. Scamehorn, J. Harwell, *Surfactant Based Separation Processes*, Marcel Dekker, New York, US **1989**.
12. E. Hinze, W. Pramauro, *Crit. Rev. Anal. Chem.* **1993**, *24*, 133.
13. F. Jiménez-Ángeles, A. Firoozabadi, *ACS Cent. Sci.* **2018**, *4*, 820.
14. R. Laurence, *Langmuir* **2006**, *22*, 32.
15. A. J. Patel, P. Varilly, S. N. Jamadagni, M. F. Hagan, D. Chandler, S. Garde, *J. Phys. Chem. B* **2012**, *116*, 2498.
16. K. Meister, S. Strazdaite, A. L. DeVries, S. Lotze, L. L. C. Olijve, I. K. Voets, H. J. Bakker, *Proc. Natl. Acad. Sci. U. S. A.* **2014**, *111*, 17732.
17. D. Laage, T. Elsaesser, J. T. Hynes, *Chem. Rev.* **2017**, *117*, 10694.
18. M. Ahmed, A. K. Singh, J. A. Mondal, *Phys. Chem. Chem. Phys.* **2016**, *18*, 2767.
19. E. Zdrali, Y. Chen, H. I. Okur, D. M. Wilkins, S. Roke, *ACS Nano* **2017**, *11*, 12111.
20. H. Schott, *Tenside, Surfactants, Deterg*. **2009**, *46*, 39.
21. D. Gokhale, I. Chen, P. S. Doyle, *Soft Matter* **2022**, *18*, 4625.
22. C. O. Rangel-Yagui, H. W. L. Hsu, A. Pessoa, L. C. Tavares, *Rev. Bras. Ciencias Farm. J. Pharm. Sci.* **2005**, *41*, 237.
23. P. Mukerjee, *J. Pharm. Sci.* **1971**, *60*, 1528.
24. G. Giorgio, G. Colafemmina, F. Mavelli, S. Murgia, G. Palazzo, *RSC Adv*. **2016**, *6*, 825.
25. P. S. Denkova, L. Van Lokeren, I. Verbruggen, R. Willem, *Society* **2008**, *112*, 10935.
26. M. Goldenberg, L. Bruno, E. Rennwantz, *J. Colloid Interface Sci.* **1993**, *158*, 351.
27. D. M. De Oliveira, S. R. Zukowski, V. Palivec, J. Hénin, H. Martinez-Seara, D. Ben-Amotz, P. Jungwirth, E. Duboué-Dijon, *Phys. Chem. Chem. Phys.* **2020**, *22*, 24014.
28. M. Ahmed, V. Namboodiri, A. K. Singh, J. A. Mondal, S. K. Sarkar, *J. Phys. Chem. B* **2013**, *117*, 16479.
29. C. I. Drexler, T. C. Miller, B. A. Rogers, Y. C. Li, C. A. Daly, T. Yang, S. A. Corcelli, P. S. Cremer, *J. Am. Chem. Soc.* **2019**, *141*, 6930.
30. J. G. Davis, K. P. Gierszal, P. Wang, D. Ben-Amotz, *Nature* **2012**, *491*, 582.
31. P. N. Perera, K. R. Fega, C. Lawrence, E. J. Sundstrom, J. Tomlinson-Phillips, D. Ben-Amotz, *Proc. Natl. Acad. Sci. U. S. A.* **2009**, *106*, 12230.
32. K. P. Gierszal, J. G. Davis, M. D. Hands, D. S. Wilcox, L. V. Slipchenko, D. Ben-Amotz, *J. Phys. Chem. Lett.* **2011**, *2*, 2930.
33. K. Mochizuki, D. Ben-Amotz, *J. Phys. Chem. Lett.* **2017**, *8*, 1360.
34. B. A. Rogers, H. I. Okur, C. Yan, T. Yang, J. Heyda, P. S. Cremer, *Nat. Chem.* **2022**, *14*, 40.
35. J. A. Long, B. M. Rankin, D. Ben-Amotz, *J. Am. Chem. Soc.* **2015**, *137*, 10809.
36. I. V. Plastinin, T. A. Dolenko, *Vib. Spectrosc.* **2022**, *123*, 103472.
37. S. Pullanchery, T. Yang, P. S. Cremer, *J. Phys. Chem. B* **2018**, *122*, 12260.
38. K. R. Vega, D. S. Wilcox, D. Ben-Amotz, *Appl. Spectrosc.* **2012**, *66*, 282.
39. X. Yang, G. Liu, L. Huo, H. Dong, H. Zhong, *Colloids Surfaces A Physicochem. Eng. Asp.* **2022**, *642*, 128589.
40. Y. Tokuoka, H. Uchiyama, M. Abe, K. Ogino, *J. Colloid Interface Sci.* **1992**, *152*, 402.
41. A. M. Al-Sabagh, N. M. Nasser, M. A. Migahed, N. G. Kandil, *Egypt. J. Pet.* **2011**, *20*, 59.
42. J. Weiss, J. N. Coupland, D. Brathwaite, D. J. McClements, *Colloids Surfaces A Physicochem. Eng. Asp.* **1997**, *121*, 53.
43. S. Karaborni, N. M. van Os, K. Esselink, P. A. J. Hilbers, *Langmuir* **1993**, *9*, 1175.

SUPPORTING INFORMATION

Additional supporting information can be found online in the Supporting Information section at the end of this article.

How to cite this article: C. M. Wentworth, R. L. Myers, P. S. Cremer, L. D. Zarzar, *Aggregate* **2023**, e385. https://doi.org/10.1002/agt2.385